

1 **Air Quality in London: Evidence of Persistence,**
2 **Seasonality and Trends**

3
4 **Luis A. Gil-Alana**

5 Faculty of Economics, University of Navarra, Pamplona, Spain

6 and

7 Universidad Francisco de Vitoria, Spain

8 Email address: alana@unav.es

9
10 **OlaOluwa S. Yaya**

11 Environmental Statistics Unit, Department of Statistics, University of Ibadan, Ibadan,

12 Nigeria & Centre for Econometric and Allied Research, University of Ibadan, Ibadan,

13 Nigeria

14 Email address: os.yaya@ui.edu.ng; o.s.olaoluwa@gmail.com

15
16 **Nieves Carmona-González**

17 Universidad Francisco de Vitoria, Spain

18 Email address: n.carmona@ufv.es

19
20 **ABSTRACT**

21 The poor air quality in the London metropolis has sparked our interest in studying the
22 time series dynamics of air pollutants in the city. The dataset consists of roadside and
23 background air quality for seven standard pollutants: nitric oxide (NO), nitrogen dioxide
24 (NO₂), oxides of nitrogen (NO_x), ozone (O₃), particulate matter (PM₁₀ and PM_{2.5}) and
25 sulphur dioxide (SO₂), using fractional integration to investigate issues such as
26 persistence, seasonality and time trends in the data. Though we notice a large degree of
27 heterogeneity across pollutants and a persistent behaviour based on a long memory
28 pattern is observed practically in all cases. Seasonality and decreasing linear trends are
29 also found in some cases. The findings in the paper may serve as a guide to air pollution
30 management and European Union (EU) policymakers.

31 **Keywords:** Air quality; time trends; long memory; fractional integration; seasonality;
32 London

33
34 **JEL Classification:** C22, Q53, Q58

35
36 Prof. Luis A. Gil-Alana gratefully acknowledges financial support from the MINEIC-AEI-FEDER
37 ECO2017-85503-R project from 'Ministerio de Economía, Industria y Competitividad' (MINEIC),
38 'Agencia Estatal de Investigación' (AEI) Spain and 'Fondo Europeo de Desarrollo Regional' (FEDER). He
39 also acknowledges support from an internal Project of the Universidad Francisco de Vitoria. Comments
40 from the Editor and two anonymous reviewers are gratefully acknowledged.

43 **1. INTRODUCTION**

44 The quality of air in London has improved significantly over the past decades (Browne et
45 al. 2007; Colette et al. 2011; EEA 2017; Andrade et al. 2018; Lang et al. 2019), but
46 exceedances of the legislative limit values still persist in some pollutants such as ozone
47 (O₃), nitrogen dioxide (NO₂) and particulate matters (PM₁₀ and PM_{2.5}), in both
48 background and roadside datasets. London failed to meet the air quality European Union
49 (EU) standard since 2010, largely due to diesel vehicles on its roads which resulted in
50 high emissions of NO₂, and congestion has further compounded the effect of diesel fumes
51 in the city. Diesel engines release NO_x, and large concentrations of NO₂ are experienced
52 along roadsides in urban areas (Gardner and Dorling 1999; Font and Fuller 2016).

53 In 2016, 43 breaches of annual pollution were recorded in London. In 2017, the
54 first breach of annual pollution limits was experienced in London, less than 10 days into
55 the New Year, and this continued for about a month into 2018. However, for the first
56 three months in 2010, no breach occurred (King's College, 2019). Currently, people in
57 London still live under poor air quality, however, NO₂ levels are falling and could reach
58 the normal level for living in the next six years. The NO₂ and particulate matters exceed
59 the EU standard, particularly during winter and early spring, not only in London but also
60 in many other European cities (Bessagnet et al. 2005; Petit et al. 2017; etc.). Based on the
61 rate of reduction in NO₂ between 2010 and 2016, Font et al. (2019) estimated that it would
62 take about 193 years for NO₂ to reach legal levels.

63 The pollution has both health and social care costs, estimated to reach about £5.3
64 billion by 2035 (O'Hare 2018). This author further reported that the costs of air pollution
65 in 2017 to the National Health Service (NHS) and social care were estimated at about
66 £157 million. The research further predicted about 2.5 million new cases of coronary
67 heart diseases, strokes, childhood cancer, lung cancer, pulmonary disease, diabetes, low

68 birth weight and dementia by 2035. Fine particulate matter ($PM_{2.5}$) and NO_2 are
69 particularly responsible for these costs. $PM_{2.5}$ is made up of particles with a diameter of
70 less than 2.5 microns. These are emitted during the combustion of vehicle engine fuels,
71 braking and tyre wearing, while NO_2 is released during the burning of fossil fuels,
72 particularly diesel fuel. Both pollutants have been targeted by the UK government,
73 seeking a strategy to reduce their exceedances. The Brexit deal could further challenge
74 London's fight to improve the quality of air since the EU has stricter standards and rules
75 than the UK is obliged to meet. Hence, concern is rising in the minds of dwellers
76 regarding the future of London's air. Air pollution has proved to be stubborn in its
77 behaviour, even if vehicle numbers are curbed, aircraft and agricultural pollution could
78 prove more of a challenge to inhabitants, and further damage human health. There is a
79 need to investigate the dynamics of the evolution of the chemistry of air pollution since
80 this will provide recommendations to modellers and predictors on the appropriate models
81 to employ in the analysis of air pollution in London. Also, the findings in this paper will
82 complement the management of air quality by the EU since there is a long-standing
83 tradition of using modelling techniques to support the design of air quality policies by
84 government authorities with regards to regulations on the emissions of pollutants.

85 In the present paper, we investigate the statistical properties of the data by looking
86 at issues such as persistence, seasonality and time trends in the dynamic evolution of air
87 quality chemistry in London. For this purpose, we use methods based on fractional
88 integration, which extend the classical analysis of stationarity/non-stationarity that only
89 use integer degrees of differentiation (i.e., 0 for stationarity and 1 for nonstationarity) to
90 fractional values. Thus, by allowing the differencing parameter to be a fractional number,
91 we allow for a much richer degree of flexibility in the dynamic specification of the data.

92 Studying air quality persistence, seasonality and trends inform us regarding the
93 possible change in the current trend of the time series; the level of persistence gives us an
94 idea of the impact that shocks would have on the series. In other words, it will tell us if
95 the series would soon revert to its mean level or would be further pushed away from its
96 mean path. In a highly persistent series, a shock to the series tends to persist for long
97 periods of time and the series drifts away from its historical mean path. Then, a time trend
98 indicates the general direction in which the series is moving, and the level of persistence
99 will tell us if shocks will have a transitory or a permanent effect.

100 It is noticeable that most empirical research on air pollution has focused on a type
101 of air pollutants such as NO₂, particulate matter 2.5 (PM_{2.5}) or sulphur dioxide (SO₂). The
102 air pollution is determined by the chemical compositions of the mixture of pollutants such
103 as SO₂, NO₂, carbon monoxide (CO), ozone (O₃), PM_{2.5} and PM₁₀, as detailed by the
104 World Health Organization (WHO, 2018) standards. Our research is also different from
105 other existing studies in this field as it involves datasets of standard air pollutants in
106 London.

107 The remainder of the paper is structured as follows: Section 2 presents a brief
108 review of air quality modelling, while Section 3 is devoted to the methodology used in
109 the paper. Section 4 describes the data. The empirical results are displayed in Section 5
110 and Section 6 contains some concluding comments.

111

112 **2. LITERATURE REVIEW**

113 Being able to assess and forecast the level of chemical composition of pollutants in the
114 air can help in preventing harmful effects on public health and facilitate the efficiency of
115 government policies aimed at improving air quality.

116 Most studies focus on two issues, on the one hand, seeking the connection between
117 pollution and harmful health effects; and, on the other hand, quantifying, modelling and
118 making predictions regarding air pollution by assessing the most suitable models for air
119 pollution. The present paper is more related to this second line of research.

120 Dealing with the first line of research, Schwartz and Marcus (1990), using
121 AutoRegressive Moving Average (ARMA) models, examined the connection between air
122 pollution and mortality in London in the period 1958-1972. The results of the study
123 demonstrated a high degree of correlation, in particular with SO₂. On the other hand,
124 using predictive methods, Gardner and Dorling (1999) analyzed NO_x (a combination of
125 NO and NO₂) using hourly meteorological data obtained from Central London using a
126 multilayer perceptron (MLP) neural network model. The findings in the study showed
127 that this model is more effective in modelling these pollutants compared to regression-
128 based models.

129 Atkinson et al. (1999) examined the relationship between emergency admissions
130 for respiratory problems and air pollution in London for the period from 1992 to 1994.
131 They used Poisson regressions to determine the correlation between hospital admissions
132 and the concentration of PM₁₀ and SO₂. Salini and Pérez (2006) used the same
133 methodology as Gardner and Dorling (1999), reaching similar results for the city of
134 Santiago de Chile. They found that the simple perceptron with a linear function is more
135 reliable for prediction than the persistence method; however, the function did not
136 outperform a multi-layered network in its predictability. "It can be said that when
137 nonlinear effects are not too important in modelling, multilayer networks are not
138 significantly better than perceptron. However, as in this case, when these non-linear
139 effects become important, multilayer networks are better in terms of their predictability,
140 compared to linear models" (Salini and Pérez 2006; page 290). Pan and Chen (2008),

141 using air pollution data in Taiwan, concluded that long memory AutoRegressive
142 Fractional Integrated Moving Average (ARFIMA) models are more accurate than
143 AutoRegressive Integrated Moving Average (ARIMA)-type models. Zamri et al. (2009),
144 in assessing Malaysian air pollution, applied the Box-Jenkins ARIMA approach by
145 modelling the maximum monthly chemical compositions of CO and NO₂ and showing an
146 increasing trend since the 1996 limits set by the US National Ambient Air Quality
147 Standards (NAAQS).

148 Beevers et al. (2013) combined two models for the study of pollution in London
149 during 2008. The first is the KCL urban model that provides annual predictions of the air
150 chemical compositions of NO, NO₂, O₃, PM₁₀ and PM_{2.5}. The second one is the urban air
151 quality model on a multiscale (CMAQ), which predicts air quality per hour. CMAQ is an
152 acronym for the Community Multi-Scale Air Quality Model, a sophisticated atmospheric
153 dispersion model developed by the US Environmental Protection Agency (EPA) to
154 address regional air pollution problems. An example of a regional air pollution problem
155 is a multi-state area where O₃ or PM_{2.5} levels exceed the US health standards. The use of
156 both models allows the quality of air, temporal and by source category to be predicted.
157 However, the authors addressed the difficulty of measuring factors such as exhaust
158 emissions, car braking, types of used tyres and, on the other hand, the need for a
159 sociological study that includes data on public and private transport use, education, etc.,
160 to correct the uncertainty of the models.

161 Li et al. (2017) analysed air quality in Beijing from 2014 to 2016 to validate the
162 effectiveness of the Long Short-Term Memory Neural Network Extended (LSTME)
163 model. The models used are the Spatio-temporal Deep Learning (StDL), the Time Delay
164 Neural Network (TDNN) model, the ARMA model, the Support Vector Regression
165 (SVR) model, and the traditional LSTME model and concluded that the LSTME model

166 is more effective than the other models as it is able to model time series with long-term
167 dependencies with optimal time delays (Li et al. 2017; page 1002) and to capture more
168 accurately effective space-time correlations and improving predictions. Naveen and Anu
169 (2017) studied air quality in India using ARIMA and seasonal ARIMA (SARIMA)
170 models, with the former being more effective than the latter. They also proposed the use
171 of alternative models to improve prediction.

172 Regarding the studies focusing on air pollution and health effects in London, we
173 should mention the studies of King's College London and the work of Anderson et al.
174 (1996), in which, through a Poisson's regression model, they found a causal link between
175 outdoor air pollution levels and mortality in London.

176 Our methodological approach is invariant to those in the literature, since it is based
177 on long memory processes and use fractional integration in the analysis of air quality
178 chemistry in London metropolis. Specifically, we dwelled on three properties of air
179 quality in London, that is, the persistence, seasonality and time trend. The outcome of the
180 findings in the paper would henceforth serve as eye opener to the choice of a forecasting
181 model for air quality chemistry level.

182

183 **3. METHODOLOGY**

184 Long memory is a feature in time series that indicates that observations are highly
185 dependent across time even if they are far distant apart. Many models can describe this
186 behaviour and one very popular in Econometrics is the one based on fractional
187 integration. Given a process $\{x_t, t = 0, \pm 1, \dots\}$, we say that it is fractionally integrated or
188 integrated of order d (i.e., $x_t \approx I(d)$) if after taking d -differences, the new process becomes
189 stationary $I(0)$. In other words, x_t is $I(d)$ if its d -differences are short memory including
190 here the white noise model but also the stationary ARMA-type of models.

191 Using L as the lag operator, i.e., $L^k x_t = x_{t-k}$, x_t is $I(d)$ if:

$$192 \quad (1 - L)^d x_t = u_t, \quad t = 1, 2, \dots \quad (1)$$

193 where u_t is $I(0)$ or short memory, and long memory takes places as long as the parameter
194 d is positive, which may be a fractional value. This is clearly an advantage with respect
195 the classical methods that exclusively consider integer degrees of differentiation, (usually,
196 1) and that based its statistical analysis on the unit root methods, simply distinguishing
197 between stationarity (if $d = 0$) and nonstationarity (if $d = 1$). Thus, allowing d to be
198 fractional we permit a much richer degree of flexibility in the dynamic specification of
199 the data.

200 Our selected model is the following one,

$$201 \quad y_t = \alpha + \beta t + x_t, \quad (1 - L)^d x_t = u_t, \quad t = 1, 2, \dots, \quad (2)$$

202 where y_t is the observed time series, and α and β are unknown coefficients referring,
203 respectively, to an intercept and a time trend; x_t is the regression error series, supposed to
204 be $I(d)$ and thus, u_t is an $I(0)$ process, described first as a white noise process and then
205 allowing for weak autocorrelation, in the latter case using the non-parametric spectral
206 approach of Bloomfield (1973). The latter is a model for the $I(0)$ term that is specified
207 exclusively in terms of its spectral density function and that fits extremely well in the
208 context of fractional integration. Moreover, its autocorrelation function decays
209 exponentially fast as in the AR case, but unlike the AR models, it is stationary across all
210 its values.

211 We estimate the fractional differencing parameter d along with the rest of
212 parameters in equation (2) by using the Whittle function in the frequency domain, and,
213 along with the estimates of the parameters in the model, we also presented the 95%
214 confidence intervals of the non-rejection values of d using a simple version of the tests of

215 Robinson (1994) widely employed in the empirical literature on I(d) processes. (see, e.g.,
216 Gil-Alana and Robinson 1997; Gil-Alana 2005; Gil-Alana and Trani 2019 and others).

217

218 **4. THE DATA**

219 The London monthly average air quality levels dataset was obtained from the London
220 Data website at <https://datahub.io/core/london-air-quality>, with both roadside and
221 background datasets of standard air quality chemistry such as nitric oxide (NO), nitrogen
222 dioxide (NO₂), oxides of nitrogen (NO_x), ozone (O₃), particulate matter (PM₁₀ and PM_{2.5})
223 and sulphur dioxide (SO₂). These datasets are site averages, obtained from London Air
224 Quality Network (LAQN) at:

225 <https://www.londonair.org.uk/london/asp/datadownload.asp>, at a daily frequency, and
226 representing London daily air quality level. At LAQN, there were 30 background and 14
227 roadside sites; with 130 monitoring sites in Greater London with 51 background and 79
228 roadside sites (see, Font et al., 2019). Note that not all locations measured all pollutants,
229 therefore it was more convenient to use datasets produced by the London Data website.
230 The data are measured in micrograms per cubic meter of air (ug/m³).

231 **INSERT TABLE 1 ABOUT HERE**

232 Time series ranges, as well as the corresponding number of observations of these
233 air quality chemistries, are tabulated in Table 1. We observe the commencement of
234 pollutants chemistry in 2008 for some variables, while others start in 2010 and all of them
235 end in December 2018. Plots of each air quality chemical composition are given in
236 Figures 1 and 2 for roadside and background readings, respectively. As noted in the plots
237 for NO, NO₂, NO_x and O₃, seasonality is clearly noticeable, as the highest values of ozone
238 level are found during summer periods in London (from June to August), while NO₂ and
239 PM₁₀ are at their lowest level during this period. For PM₁₀, PM_{2.5} and SO₂, in both data

240 reading sources (roadside, Figure 1 and background, Figure 2), we observe irregular time
241 dynamics, albeit with occasional long spikes mimicking seasonality in the datasets.
242 Summary statistics for the mean, minimum and maximum values of air quality chemistry
243 levels for both roadside and background readings are given in Table 2. For NO_2 , the mean
244 value for the series is above the EU standard of $40\mu\text{g}/\text{m}^3$ for the roadside readings of the
245 pollutant, while this is below the standard for the background readings ($34\mu\text{g}/\text{m}^3$),
246 whereas the maximum background value is above the standard ($60.237\mu\text{g}/\text{m}^3$). For PM_{10}
247 and $\text{PM}_{2.5}$ in the roadside readings, the maximum values are above the exceedances limit,
248 while only the $\text{PM}_{2.5}$ is above the EU standard, though the $\text{PM}_{2.5}$ is known to be more
249 hazardous. Generally, there are wide disparities between maximum and minimum air
250 pollution chemistry levels of all the seven pollutants for roadside and background
251 readings.

252 **INSERT FIGURES 1 AND 2 ABOUT HERE**

253 **INSERT TABLE 2 ABOUT HERE**

254

255 **5. EMPIRICAL RESULTS**

256 The results in Table 3 are obtained under the assumption that the error term u_t in (2) is a
257 white noise process. Thus, no autocorrelation is permitted apart from the one produced
258 by the fractional differencing structure. We display the estimates of d (and the 95%
259 confidence bands) for the three classic cases of i) no regressors, ii) with an intercept, and
260 iii) with an intercept and a linear time trend, marking in bold in the table the selected case
261 for each series depending on the significance of the coefficients based on their
262 corresponding t-values.

263 **INSERT TABLES 3 AND 4 ABOUT HERE**

264 We observe in Table 3 that the time trend coefficient is significant in a number of
 265 cases, in particular for PM_{10} and $PM_{2.5}$ in the two cases of roadside and background series.
 266 Looking at the estimates of the differencing parameter, we observe that the unit root null
 267 hypothesis, i.e., $d = 1$ cannot be rejected in the cases of NO and NO_x for the London mean
 268 roadside, and in the cases of NO_x and O_3 for the background series. In all the other cases,
 269 the estimates of d are found to be statistically significantly smaller than 1 implying mean-
 270 reverting behaviour, and for two of the series ($PM_{2.5}$ in the roadside and PM_{10} in
 271 background), the $I(0)$ hypothesis of short memory behaviour cannot be rejected, implying
 272 a very short degree of dependence between the observations in these two cases.

273 In Table 4, we allow for autocorrelation in the error term. As earlier mentioned,
 274 we use here a non-parametric approach due to Bloomfield (1973) which is quite
 275 convenient in the context of fractional integration and that approximates very well highly
 276 parameterized ARMA models with few parameters.¹ Here we observe that the time series
 277 is significant in a large number of cases and the estimated values of d are now smaller
 278 than 1 in all cases. Moreover, the $I(0)$ hypothesis cannot be rejected now in the majority
 279 of the cases, and evidence of long memory (i.e., $d > 0$) only takes place in the cases of
 280 NO for roadside and SO_2 for background. Thus, it seems that the competition between
 281 the two structural approaches (No autocorrelation and Bloomfield autocorrelation cases)
 282 is the cause of the reduction in the values of the differencing parameter. These results,
 283 however, though allowing for autocorrelation, do not take into account the potential
 284 seasonal (monthly) nature of the data. Thus, in the following table, we take this feature
 285 into consideration by allowing for a seasonal monthly AR(1) structure on u_t , i.e.,

$$286 \quad u_t = \phi u_{t-12} + \varepsilon_t, \quad t = 1, 2, \dots, \quad (3)$$

287 where ε_t is now a white noise process.

¹ See Gil-Alana (2004) for the modelization of Bloomfield (1973) in the context of fractional integration.

288 **INSERT TABLES 5 AND 6 ABOUT HERE**

289 The results using this model are presented in Table 5 with further results for
290 selected cases in Table 5 displayed in Table 6. In Table 5, the long memory feature is
291 found in the majority of the cases with the values of d belonging to the interval $(0, 1)$.
292 Evidence of short memory ($d = 0$) is only found in the cases of PM_{10} (roadside and
293 background) and $PM_{2.5}$ (roadside) particulates. Table 6 displays the estimated model
294 coefficients under the selected specification in Table 5. We observe significant seasonal
295 AR coefficients and, in those cases where the time trend is statistically significant, it is
296 found to be negative in all cases, implying a decreasing deterministic pattern in the data.
297 This is consistent with other works that also find a decreasing trend in London air
298 pollutants (e.g., Lang et al., 2019).

299 **INSERT TABLE 7 ABOUT HERE**

300 As a second approach in the analysis of the seasonality issue, we conducted
301 seasonality tests using the method detailed in Beaulieu and Miron (1993). This is
302 Hylleberg et al.'s (HEGY, 1990) test version for monthly frequency series.
303 Nonstationarity and seasonality can both be tested in this approach simultaneously,
304 following Box, Jenkins and Reinsel (2008) who proposed carrying out the lag operation
305 $(1 - L^s)x_t$ for seasonal differencing in order to obtain a transformed stationary weakly
306 dependent series. For monthly data, as in our case, $s = 12$. The Seasonal Monthly
307 Integration (SMI) process representing such a time series is,

308
$$(1 - L^{12})x_t = u_t, \quad t = 1, 2, \dots \quad (4)$$

309 where all the 12 roots lie within the unit circle. Using then the decomposition $(1 - L^{12}) =$
310 $(1 - L)\phi(L)$, where $\phi(L) = (1 + L + L^2 + \dots + L^{11})$, the first of these components, $(1 - L)$
311 is related to the regular (zero frequency) unit root test using the t_1 statistic, which is
312 equivalent to the classical ADF unit root test. The remaining factors are then used in the

313 seasonal unit root testing, while at annual frequency, the t statistic t_2 is used in testing
 314 annual seasonal unit roots. For all other frequencies, the joint test for seasonal unit root
 315 at any data frequency is carried out using the F test statistic F_{2-12} . (Details on HEGY
 316 testing procedure for monthly frequency dataset is found in Beaulieu and Miron 1993).

317 We conducted the HEGY test for the cases of i) an intercept only, ii) an intercept
 318 with a linear time trend and iii) with an intercept, a trend and seasonal dummies. The
 319 results are presented in Table 7 with the unit root test results for roadside readings
 320 presented in the upper panel (i) and those of background readings presented in the lower
 321 panel (ii). The results indicate non-rejection of the null hypotheses for non-seasonal unit
 322 root and seasonal unit root tests, for intercept only and an intercept with trend, based on t
 323 statistics t_1 and t_2 , implying evidence of regular unit root and annual seasonal unit roots
 324 in the series. For all other frequencies other than the zero frequency (non-seasonal
 325 frequency), we conducted F tests F_{2-12} and these are significant throughout, implying that
 326 seasonality is only detected at the annual frequency but it is not found at any other
 327 frequency.

328 As a final step, we also examined the possibility of non-linear trends with smooth
 329 breaks, still within the context of fractional integration, and for this purpose, we used the
 330 method proposed in Cuestas and Gil-Alana (2016) which is based on the Chebyshev's
 331 polynomials in time.² In particular, we consider here the following model,

$$332 \quad y_t = \sum_{i=0}^m \theta_i P_{iT}(t) + x_t; \quad (1 - L)^d x_t = u_t, \quad t = 1, 2, \dots, \quad (5)$$

333 with m indicating the order of the Chebyshev polynomial $P_{iT}(t)$ defined as:

$$334 \quad P_{0,T}(t) = 1,$$

² This nonlinear deterministic function allows for modelling smooth breaks in the time series. It is similar in application to flexible Fourier function of Enders and Lee (2012a,b), recently applied in fractional integration framework in Gil-Alana and Yaya (2020).

335
$$P_{i,T}(t) = \sqrt{2} \cos(i\pi(t-0.5)/T), \quad t = 1, 2, \dots, T; \quad i = 1, 2, \dots \quad (6)$$

336 Hamming (1973) and Smyth (1998) showed detailed descriptions of these polynomials
 337 in time, and Bierens (1997) and Tomasevic and Stanivuk (2009) argued that it is possible
 338 to approximate highly non-linear trends with low degree polynomials. Thus, if $m = 0$ in
 339 (5), the model contains an intercept; if $m = 1$ it also includes a linear trend; and if $m > 1$
 340 it becomes non-linear - the higher m is, the less linear the approximated deterministic
 341 component becomes. For our dataset, we set $m = 3$ and thus, significant values of the
 342 estimates of θ_2 and/or θ_3 will provide us with evidence of non-linearity.

343 **INSERT TABLE 8 ABOUT HERE**

344 Table 8 reproduces the results under the assumption that u_t in (5) is a white noise
 345 process, though almost identical results were obtained under weak (seasonal and non-
 346 seasonal) autocorrelation. The first thing we observe in this table is that there are very
 347 few cases of non-linearities. In fact, only for PM_{10} under the roadside series, and for SO_2
 348 in the background reading do we find significant parameter estimates θ_2 and/or θ_3 ,
 349 implying nonlinearity of series dynamics. Focussing on the estimates of d , the results
 350 once more indicate some shreds of evidence of long memory patterns. Starting with the
 351 background case, there is a single case of a short memory pattern, i.e., $d = 0$ (PM_{10}); four
 352 series with values of d constrained between 0 and 1: SO_2 , ($d = 0.15$), $PM_{2.5}$ (0.24), NO ,
 353 (0.67) and NO_2 , (0.68); and finally, there are two cases where the unit root null, i.e., $d =$
 354 1 cannot be rejected: NO_x , (0.74) and O_3 , (0.83). For the roadside series, evidence of $I(0)$
 355 behaviour is found in the two PM particulates (PM_{10} and $PM_{2.5}$). The unit root hypothesis
 356 cannot be rejected for NO , (with $d = 0.73$), and evidence of long memory with d ranging
 357 between 0 and 1 is obtained for the remaining cases.

358

359

360 6. CONCLUSIONS

361 The analyses carried out in this article and its results are transcendent as they examined
362 the air quality in London by providing evidence of persistence, seasonality and time
363 trends in various air quality pollutants. In particular, we have examined two datasets,
364 these being roadside and background standard air quality chemistry readings such as nitric
365 oxide, nitrogen dioxide, oxides of nitrogen, ozone, particulate matter (PM₁₀ and PM_{2.5})
366 and sulphur dioxide. Our results indicate that long memory is present in the majority of
367 the cases, implying high degrees of persistence measured in terms of a fractional
368 differencing parameter that is constrained between 0 and 1. Mean reversion is also found
369 practically in all cases since the values are found to be significantly smaller than 1. This
370 means that shocks will tend to disappear by themselves in the long run. Seasonality is
371 another relevant factor and the time trend if significant, is found to be negative in all cases
372 indicating a reduction in pollutant levels.

373 The evidence of long memory is consistent with numerous other works that found
374 this feature in many other disciplines including hydrology (Hurst, 1951), climatology
375 (Gil-Alana, 2005; Rea et al., 2011; Gil-Alana and Sauci, 2019), environmental sciences
376 (Barassi et al., 2011; Belbute and Pereira, 2017; Gil-Alana and Trani, 2019), etc. On the
377 other hand, seasonality is something to be expected due to the monthly frequency of the
378 data and the mixing layer dynamics, meteorological conditions and emission patterns.

379 The possibility of structural breaks has not been considered in this work. This is
380 an important issue, noting that several authors have shown that fractional integration and
381 structural breaks are very much related (Diebold and Inoue, 2001; Granger and Hyung,
382 2004; Ohanissian et al., 2008; etc.). Instead of that and based on the small number of
383 observations used in this application, we have considered a nonlinear approach based on
384 Chebyshev polynomials in time, and that approximates breaks in a rather smooth way.

385 The fractional integration modelling framework can easily be generalized to the
386 Seasonal Autoregressive Fractionally Integrated Moving Average (SARFIMA) model or
387 other variants which allow for forecasting values of the chemical composition of air
388 quality, but the outcome of these findings would have served as eye opener to the choice
389 of forecasting model, other than the SARFIMA model.³ The findings could further help
390 in the designing of environmental policies aimed at challenging and further reducing
391 atmospheric pollution by 2050 in line with the UN 2030 Agenda, which focuses on the
392 Sustainable Development Goals. It is essential to redesign the management of air
393 pollution in London by focusing on improving emissions mainly from transportation.
394 Also, appropriate measures should be taken in each seasonal quarter of London's weather
395 since air quality is at its poorest level during the summer. This is because the tropospheric
396 ozone, unlike other pollutants, is not emitted directly into the atmosphere, but it is a
397 secondary pollutant produced by the reaction between nitrogen dioxide, hydrocarbons
398 and sunlight; therefore, high levels of ozone pollution take place in the central hours of
399 the day during the summer.

400
401 **The data that support the findings of this study are openly available in the London**
402 **Data website at <https://datahub.io/core/london-air-quality>**
403

404

405

406

References

407

408 Anderson HR, Ponce de Leon A, Martin-Bland J, Bower J.S., Strachan DP (1996) Air
409 pollution and daily mortality in London: 1987-92, *BMJ* 312:665-669.
410 <http://doi:10.1136/bmj.312.7032.665>

411

412 Andrade CJS, Dameno A, Perez J, Lumbreras J (2018). Implementing city-level carbon
413 accounting: A Comparison between Madrid and London. *J Cleaner Prod* 172: 795-804.
414 [https://doi: DOI:10.1016/j.jclepro.2017.10.163](https://doi:DOI:10.1016/j.jclepro.2017.10.163)

415

416 Atkinson RW, Anderson HR, Strachan DP, Bland JM, Bremner SA, Ponce de Leon A
417 (1999) Short-term associations between outdoor air pollution and visits to accident and

³ Forecasting with seasonal and non-seasonal fractionally integrated models has been examined among others by Wang and Hsiao (2013), Vera-Valdes (2020) and Bisaglia and Grigoletto (2020).

418 emergency departments in London for respiratory complaints *Eur Respir J* 13(2):257–
419 265.
420 [http://doi: 10.1183/09031936.99.1322579](http://doi:10.1183/09031936.99.1322579)
421
422 Barassi MR, Cole MA and Elliott RJR (2011) The stochastic convergence of CO₂
423 emissions: A long memory approach. *Environ Resource Econ* 49:367-385.
424 <https://doi.org/10.1007/s10640-010-9437-7>
425
426 Beaulieu JJ, Miron JA (1993) Seasonal unit roots in aggregate US data. *J Econometrics*
427 55:305–328.
428 [https://doi.org/10.1016/0304-4076\(93\)90018-Z](https://doi.org/10.1016/0304-4076(93)90018-Z)
429
430 Bessagnet B, Hodzic A, Blanchard O, Lattuat M, Le Bihan O, Marfaing H, Rouil L
431 (2005) Origin of particulate matter pollution episodes in wintertime over the Paris Basin.
432 *Atmos Environ* 39:6159-6174.
433 <https://doi.org/10.1016/j.atmosenv.2005.06.053>
434
435 Beevers S, Nutthida K., Williams M, Kelly F, Anderson H, Carslaw D (2013) Air
436 pollution dispersion models for human exposure predictions in London. *J Expo Sci Env*
437 *Epi* 23:647–653.
438 [http://doi: 10.1038/jes.2013.6](http://doi:10.1038/jes.2013.6)
439
440 Belbute JM, Pereira AM (2017) Do global CO₂ emissions from fossil-fuel consumption
441 exhibit long memory? A fractional integration analysis. *Appl Econ* 49:4055-4070.
442 <https://doi.org/10.1080/00036846.2016.1273508>
443
444 Bierens HJ (1997) Testing the unit root with drift hypothesis against nonlinear trend
445 stationarity with an application to the US price level and interest rate. *J Econometrics*
446 81:29-64.
447 [https://doi.org/10.1016/S0304-4076\(97\)00033-X](https://doi.org/10.1016/S0304-4076(97)00033-X)
448
449 Bisaglia, L. and M. Grigoletto, (2020), A new time varying model for forecasting long
450 memory series, *Statistical Methods and Applications*, forthcoming
451 <https://doi.org/10.1007>
452
453 Bloomfield P (1973) An exponential model in the spectrum of a scalar time series.
454 *Biometrika* 60:217-226.
455 [https://doi: 10.1093/biomet/60.2.217](https://doi:10.1093/biomet/60.2.217).
456
457 Box GEP, Jenkins GM, Reinsel GC (2008) *Time Series Analysis: Forecasting and*
458 *Control*, 4th ed. Wiley: Hoboken, New Jersey.
459 <https://doi.org/10.1111/jtsa.12194>
460
461 Browne M, Allen J, Anderson S (2007). Low emission zones: the likely effects on the
462 freight transport sector. *Int J Logist-Res App* 8(4): 269-281.
463 <https://doi.org/10.1080/13675560500405899>
464
465 Colette et al. (2011). Air quality trends in Europe over the past decade: a first multi-model
466 assessment. *Atmos Physics*, 11: 11657-11678.
467 <https://doi.org/10.5194/acp-11-11657-2011>

468
469 Cuestas JC, Gil-Alana LA (2016) A non-linear approach with long range dependence
470 based on Chebyshev polynomials. *Stud Nonlinear Dyn E* 20,1: 57-94.
471 <https://doi.org/10.1016/j.qref.2020.01.007>
472
473 Diebold F.X., Inoue A (2001). Long memory and regime switching. *Journal of*
474 *Econometrics* 105, 131-159. [https://doi.org/10.1016/S0304-4076\(01\)00073-2](https://doi.org/10.1016/S0304-4076(01)00073-2)
475
476 EEA (2017), European Environment Agency: Air quality in Europe, n° 13/2017.
477
478 Enders W, Lee J (2012a) A unit root test using a Fourier series to approximate smooth
479 breaks. *Oxford Bulletin of Economics and Statistics*, 74: 574-599.
480 <https://doi.org/10.1111/j.1468-0084.2011.00662.x>
481
482 Enders W, Lee J (2012b). The flexible Fourier form and Dickey-Fuller-type unit root
483 tests. *Economic Letters*, 117: 196-199. <https://doi.org/10.1016/j.econlet.2012.04.081>
484
485 Font A, Fuller GW (2016) Did policies to abate atmospheric emissions from traffic have
486 a positive effect in London?. *Environ Pollut* 218:463-474.
487 <https://doi:10.1016/j.envpol.2016.07.026>
488
489 Font A, Guiseppin L, Blangiardo M, Ghersi V, Fuller GW (2019) A tale of two cities: is
490 air pollution improving in Paris and London?. *Environ Pollut* 249:1-12.
491 <https://doi.org/10.1016/j.envpol.2019.01.040>
492
493 Franses PH, Hobijn B (1997). Numbers from all the tables in critical values for unit root
494 tests in seasonal time series. *J Appl Stat* 24:25-46.
495 <https://doi.org/10.1080/02664769723864>
496
497 Gardner MW, Dorling SR (1999) Neural network modelling and prediction of hourly
498 NO_x and NO₂ concentrations in urban air in London. *Atmos Environ* 33:709-719.
499 [https://doi.org/10.1016/S1352-2310\(98\)00230-1](https://doi.org/10.1016/S1352-2310(98)00230-1)
500
501 Gil-Alana LA (2004) The case of Bloomfield (1973) model as an approximation to
502 ARMA processes in the context of fractional integration, *Mathematical and Computer*
503 *Modelling* 39:429 – 436.
504 [https://doi:10.1016/S0895-7177\(04\)90515-8](https://doi:10.1016/S0895-7177(04)90515-8)
505
506 Gil-Alana LA (2005) Statistical model for the temperatures in the Northern hemisphere
507 using fractional integration techniques. *J Climate*, 18(24): 5537-5369.
508 <https://doi.org/10.1175/JCLI3543.1>
509
510 Gil-Alana LA, Robinson PM (1997) Testing of unit roots and other nonstationary
511 hypotheses in macroeconomic time series. *J Econometrics* 80:241-268.
512 <https://doi.org/10.1016/S0304-4076>.
513
514 Gil-Alana LA, Sauci L (2019) Temperatures across Europe. Evidence of time trends,
515 *Clim Change* 157(3): 355-364.
516 <https://doi:10.1007/s10584-019-02568-6>
517

518 Gil-Alana LA, Trani T (2019) Time Trends and Persistence in the Global CO₂ Emissions
519 across Europe. *Environ Resource Econ* 73:213-228.
520 <https://doi.org/10.1007/s10640-018-0257-5>
521

522 Gil-Alana, LA, Yaya OS (2020) Testing Fractional Unit Roots with Non-linear Smooth
523 Break Approximations using Fourier functions. *Journal of Applied Statistics*.
524 <https://doi.org/10.1080/02664763.2020.1757047>
525

526 Granger C.W.J and Hyung N (2004). Occasional structural breaks and long memory with
527 an application to the S&P 500 absolute stock returns. *Journal of Empirical Finance*,11:
528 399-421.
529 <https://doi.org/10.1016/j.jempfin.2003.03.001>
530

531 Hamming RW (1973) *Numerical Methods for Scientists and Engineers*, Mineola, New
532 York: Dover Publications.
533

534 Hurst HE (1951) Long-term storage capacity of reservoirs. *Trans Am Soc Civil Eng*
535 116:770-799.
536

537 Hylleberg S, Engle RF, Granger CWJ, Yoo BS (1990). Seasonal integration and
538 cointegration. *J Econometrics* 44: 215 – 238.
539 [https://doi.org/10.1016/0304-4076\(90\)90080-D](https://doi.org/10.1016/0304-4076(90)90080-D)
540

541 King's College (2019). [https://kclpure.kcl.ac.uk/portal/en/persons/sean-beevers](https://kclpure.kcl.ac.uk/portal/en/persons/sean-beevers(69d4f8e7-56f5-4751-84e3-2d735371f03e)/publications.html)
542 [\(69d4f8e7-56f5-4751-84e3-2d735371f03e\)/publications.html](https://kclpure.kcl.ac.uk/portal/en/persons/sean-beevers(69d4f8e7-56f5-4751-84e3-2d735371f03e)/publications.html). Accessed 12 October
543 2019.
544

545 Lang PE, Carslaw DC, Moller SJ (2019). A trend analysis approach for air quality
546 network data, *Atmos Environ* 2, forthcoming.
547 <https://doi.org/10.1016/j.aeaoa.2019.100030>
548

549 Li X, Peng L, Yao X, Cui S, Hi Y, You C, Chi T (2017). Long short-term memory neural
550 network for air pollutant concentration predictions: Method development and evaluation.
551 *Environ Pollut* 231:1997-1004.
552 <https://doi.org/10.1016/j.envpol.2017.08.114>
553

554 Naveen V, Anu N (2017) Time series analysis to forecast air quality indices in
555 Thiruvananthapuram District, Kerala, India. *J Eng Res Appl* 7(6): 66-84.
556 <https://doi.org/10.9790/9622-0706036684>
557

558 Ohanissian, A. J.R. Russell and R.S. Tsay (2008), True or spurious long memory? A new
559 test. *Journal of Business and Economic Statistics*, 26, 161-175.
560 <https://doi.org/10.1198/073500107000000340>
561

562 O'Hare R (2018) Air pollution in England could cost as much as £5.3 billion by 2035.
563 Published 22 May 2018. [https://www.imperial.ac.uk/news/186406/air-pollution-england-](https://www.imperial.ac.uk/news/186406/air-pollution-england-could-cost-much/)
564 [could-cost-much/](https://www.imperial.ac.uk/news/186406/air-pollution-england-could-cost-much/). Accessed 10 September 2019.
565

566 Pan JN, Chen ST (2008) Monitoring long-memory air quality data using ARFIMA model,
567 *Environmetrics* 19 (2): 209–219.

568 <https://doi.org/10.1002/env.88>
569
570 Petit JE, Amodeo T, Meleux F, Bessagnet B, Menut L, Grenier D, Favez O (2017)
571 Characterising an intense PM pollution episode in March 2015 in France from multi-site
572 approach and near real time data: Climatology, variabilities, geographical origins and
573 model evaluation. *Atmos Environ* 155: 68-84.
574 <https://doi.org/10.1016/j.atmosenv.2017.02.012>
575
576 Rea, W., M. Reale and J. Brown (2011), Long memory in temperature reconstructions,
577 *Clim Change* 107(3-4): 247-265.
578 <https://doi.org/10.1007/s10584-011-0068-y>
579
580 Robinson PM (1994) Efficient tests of nonstationarity hypotheses. *J Am Stat Assoc*
581 89:1420–1437.
582 <https://doi.org/10.1080/01621459>
583
584 Salini G, Pérez P (2006) Time series analysis of atmosphere pollution data using artificial
585 neural networks techniques. *Ingeniare* 14:284-290.
586 <http://dx.doi.org/10.4067/S0718-3305>
587
588 Schwartz O, Marcus A (1990) Mortality and air pollution in London: A time series
589 analysis. *Am J Epidemiol* 131(1):185–194.
590 <https://doi.org/10.1136/jech.54.10.750>
591
592 Smyth GK (1988) *Polynomial Approximation*. John Wiley & Sons, Ltd, Chichester,
593 (1998).
594 <https://doi.org/10.1002/9781118445112.stat05031>
595
596 Tomasevic NM, Stanivuk T (2009) Regression Analysis and approximation by means of
597 Chebyshev Polynomial, *Informatologia* 42:166-172.
598
599 Vera-Valdes, E., (2020) On long memory origins and forecast horizons, *Journal of*
600 *Forecasting*, forthcoming. DOI: 10.1002/for.2651
601
602 Wang, C.S.H. and C. Hsiao (2013), Forecasting a long memory process subject to
603 structural breaks, *Journal of Econometrics* 177, 2, 171-184.
604 <https://doi.org/10.1016/j.jeconom.2013.04.006>
605
606 World Health Organization (2018), Air pollution, [https://www.who.int/news-room/fact-](https://www.who.int/news-room/fact-sheets/detail/ambient-(outdoor)-air-quality-and-health)
607 [sheets/detail/ambient-\(outdoor\)-air-quality-and-health](https://www.who.int/news-room/fact-sheets/detail/ambient-(outdoor)-air-quality-and-health). Accessed 12 October 2019.
608
609 Zamri IM, Roziah Z, Marzuki I, Muhd SL (2009) Forecasting and Time Series Analysis
610 of Air Pollutants in Several Area of Malaysia. *Am J Environ Sci* 5:625-632.
611 <https://doi.org/10.3844/ajessp.2009.625.632>
612
613

614 **Table 1: Time series of London Air Quality**

| London mean roadside | | | |
|-------------------------------------|-----------------|---------------|------------|
| Series | Starting period | Ending period | N. of Obs. |
| Nitric oxide, NO | January 2010 | December 2018 | 108 |
| Nitrogen dioxide, NO ₂ | January 2008 | December 2018 | 132 |
| Oxides of nitrogen, NO _x | January 2010 | December 2018 | 108 |
| Ozone, O ₃ | January 2008 | December 2018 | 132 |
| PM ₁₀ particulate | January 2008 | December 2018 | 132 |
| PM _{2.5} particulate | January 2008 | December 2018 | 132 |
| Sulphur dioxide, SO ₂ | January 2008 | December 2018 | 132 |
| London mean background | | | |
| Nitric oxide, NO | January 2010 | December 2018 | 108 |
| Nitrogen dioxide, NO ₂ | January 2008 | December 2018 | 132 |
| Oxides of nitrogen, NO _x | January 2010 | December 2018 | 108 |
| Ozone, O ₃ | January 2008 | December 2018 | 132 |
| PM ₁₀ particulate | January 2008 | December 2018 | 132 |
| PM _{2.5} particulate | May 2008 | December 2018 | 128 |
| Sulphur dioxide, SO ₂ | January 2008 | December 2018 | 132 |

615

616

617

618 **Table 2: Data Summary**

| Series | London mean roadside | | | London mean background | | |
|-------------------------------------|----------------------|------------|------------|------------------------|------------|------------|
| | Mean | Min. value | Max. Value | Mean | Min. value | Max. value |
| Nitric oxide, NO | 78.339 | 27.211 | 180.933 | 22.123 | 4.172 | 79.245 |
| Nitrogen dioxide, NO ₂ | 55.757 | 38.950 | 75.922 | 34.865 | 20.050 | 60.237 |
| Oxides of nitrogen, NO _x | 139.490 | 82.235 | 250.743 | 56.383 | 25.642 | 129.152 |
| Ozone, O ₃ | 27.174 | 10.658 | 46.266 | 36.895 | 13.869 | 62.562 |
| PM ₁₀ particulate | 25.122 | 16.285 | 43.315 | 19.272 | 11.927 | 36.933 |
| PM _{2.5} particulate | 15.715 | 7.898 | 32.581 | 13.293 | 6.395 | 29.912 |
| Sulphur dioxide, SO ₂ | 3.263 | -1.687 | 8.541 | 3.362 | 1.079 | 6.734 |

619 The Air Quality Standards Regulations 2010 is found at
620 <http://www.legislation.gov.uk/uksi/2010/1001/schedule/2/made>. This documents the safe limits for NO₂
621 as 40 µg/m³. For PM₁₀ and PM_{2.5}, they are 40 µg/m³ and 25 µg/m³, respectively.

622

623

624

625

626

627

628

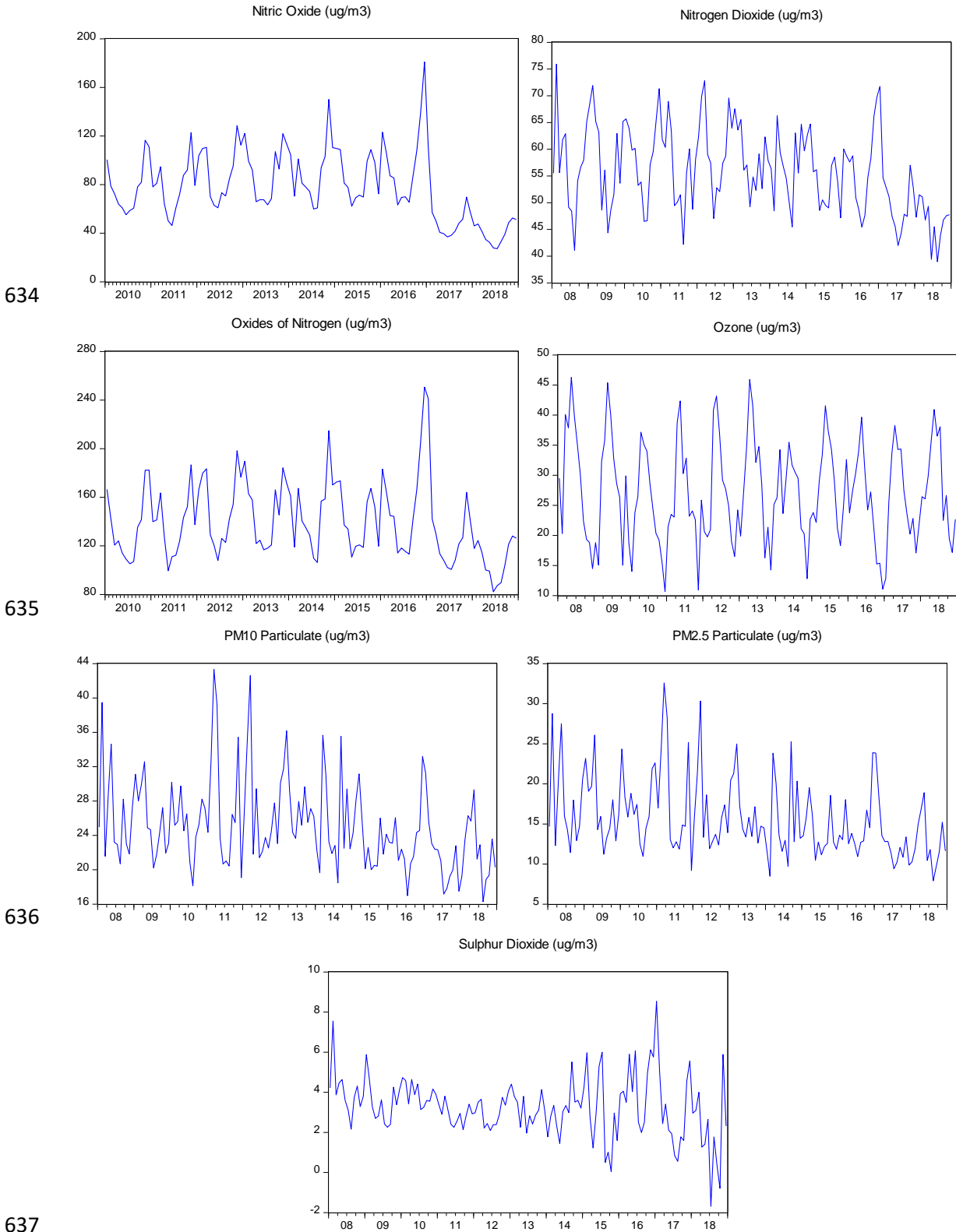
629

630

631

632

633



634

635

636

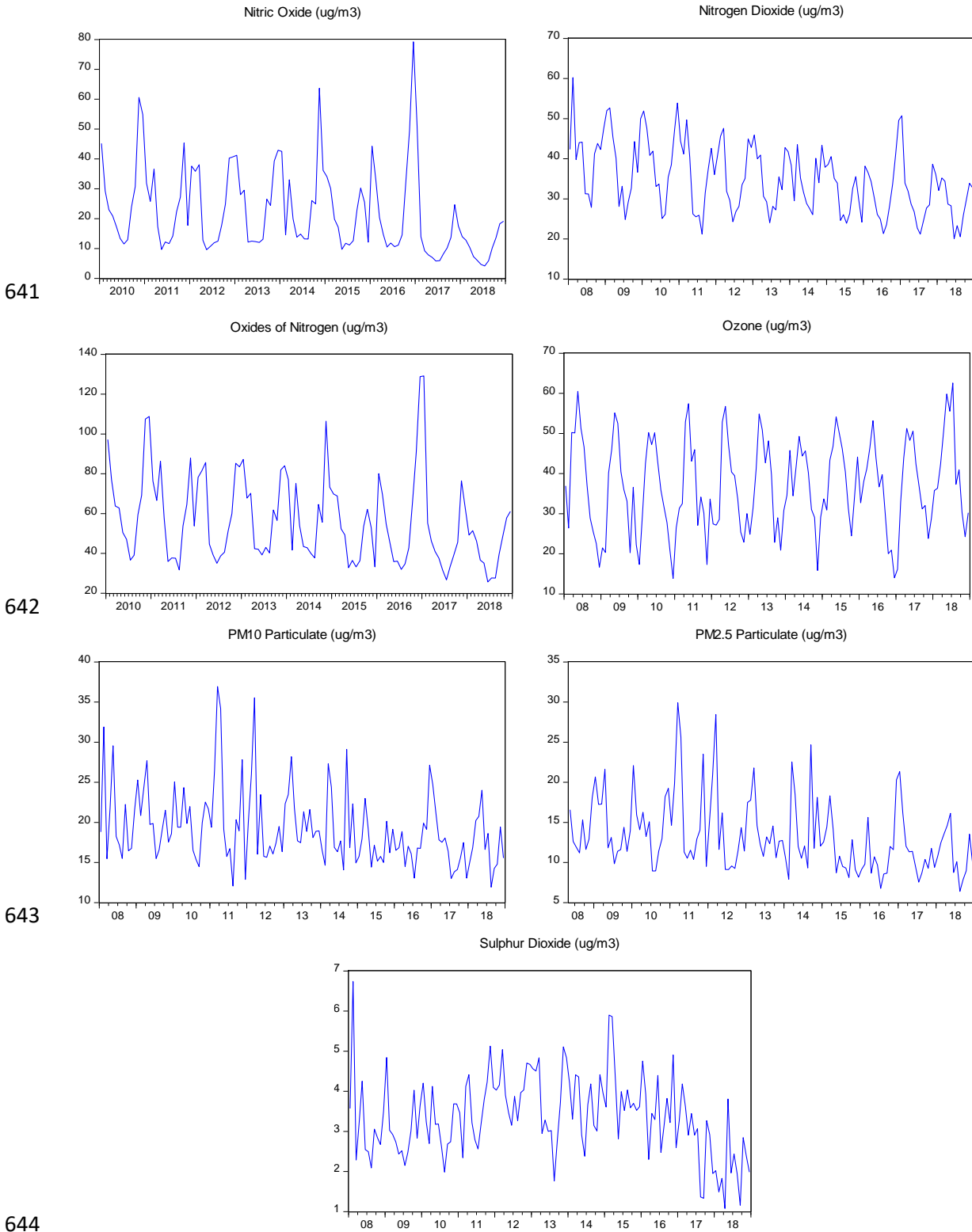
637

638

639

640

Figure 1: London Mean Roadside Air Quality readings on y-axis, measured in ug/m³ and plotted year, the x-axis of each plot.



641

642

643

644

645

646

647

Figure 2: London Mean Background Air Quality readings on y-axis, measured in ug/m^3 and plotted year, the x-axis of each plot.

648 **Table 3: Estimates of d under the assumption of no autocorrelation**

| London mean roadside | | | |
|-------------------------------------|-------------------|--------------------------|---------------------------|
| Series | No terms | With intercept | With a time trend |
| Nitric oxide, NO | 0.72 (0.62, 1.00) | 0.76 (0.56, 1.03) | 0.76 (0.55, 1.03) |
| Nitrogen dioxide, NO ₂ | 0.82 (0.70, 0.99) | 0.50 (0.34, 0.70) | 0.48 (0.31, 0.70) |
| Oxides of nitrogen, NO _x | 0.79 (0.63, 1.00) | 0.73 (0.50, 1.00) | 0.73 (0.50, 1.00) |
| Ozone, O ₃ | 0.80 (0.63, 1.01) | 0.74 (0.51, 0.98) | 0.74 (0.51, 0.98) |
| PM ₁₀ particulate | 0.58 (0.46, 0.72) | 0.24 (0.12, 0.41) | 0.18 (0.04, 0.39) |
| PM _{2.5} particulate | 0.48 (0.36, 0.63) | 0.23 (0.12, 0.39) | 0.12 (-0.06, 0.35) |
| Sulphur dioxide, SO ₂ | 0.46 (0.31, 0.64) | 0.31 (0.17, 0.50) | 0.31 (0.16, 0.50) |
| London mean background | | | |
| Series | No terms | With intercept | With a time trend |
| Nitric oxide, NO | 0.69 (0.48, 0.95) | 0.67 (0.42, 0.98) | 0.68 (0.42, 0.98) |
| Nitrogen dioxide, NO ₂ | 0.87 (0.72, 1.07) | 0.68 (0.47, 0.93) | 0.68 (0.45, 0.93) |
| Oxides of nitrogen, NO _x | 0.77 (0.58, 1.01) | 0.73 (0.46, 1.02) | 0.74 (0.47, 1.02) |
| Ozone, O ₃ | 0.85 (0.67, 1.07) | 0.83 (0.60, 1.07) | 0.83 (0.60, 1.07) |
| PM ₁₀ particulate | 0.52 (0.40, 0.66) | 0.20 (0.09, 0.38) | 0.12 (-0.06, 0.35) |
| PM _{2.5} particulate | 0.49 (0.37, 0.64) | 0.31 (0.18, 0.51) | 0.27 (0.08, 0.50) |
| Sulphur dioxide, SO ₂ | 0.47 (0.34, 0.62) | 0.33 (0.24, 0.46) | 0.33 (0.24, 0.46) |

649 In bold, the significant cases according to the deterministic terms. In parenthesis, the 95% confidence
650 intervals of the values of d.

651

652

653 **Table 4: Estimates of d under the assumption of autocorrelation**

| London mean roadside | | | |
|-------------------------------------|---------------------|----------------------------|----------------------------|
| Series | No terms | With intercept | With a time trend |
| Nitric oxide, NO | 0.51 (0.22, 0.91) | 0.35 (0.15, 0.76) | 0.32 (0.11, 0.76) |
| Nitrogen dioxide, NO ₂ | 0.71 (0.51, 0.99) | 0.24 (0.03, 0.73) | 0.15 (-0.11, 0.73) |
| Oxides of nitrogen, NO _x | 0.54 (-0.03, 0.98) | 0.18 (-0.10, 0.74) | 0.14 (-0.13, 0.74) |
| Ozone, O ₃ | 0.32 (-0.12, 1.04) | -0.26 (-0.57, 0.73) | -0.23 (-0.58, 0.73) |
| PM ₁₀ particulate | 0.51 (-0.06, 0.76) | 0.07 (-0.06, 0.27) | -0.10 (-0.26, 0.27) |
| PM _{2.5} particulate | 0.45 (-0.13, 0.70) | 0.09 (-0.05, 0.30) | -0.37 (-0.59, 0.30) |
| Sulphur dioxide, SO ₂ | 0.28 (-0.14, 0.73) | 0.02 (-0.24, 0.39) | 0.03 (-0.23, 0.39) |
| London mean background | | | |
| Series | No terms | With intercept | With a time trend |
| Nitric oxide, NO | -0.01 (-0.19, 0.67) | 0.00 (-0.23, 0.76) | -0.18 (-0.47, 0.45) |
| Nitrogen dioxide, NO ₂ | 0.59 (0.35, 0.96) | 0.17 (-0.01, 0.73) | -0.43 (-0.81, 0.83) |
| Oxides of nitrogen, NO _x | -0.12 (-0.19, 0.89) | -0.08 (-0.34, 0.74) | -0.46 (-1.04, 0.58) |
| Ozone, O ₃ | -0.05 (-0.11, 1.11) | -0.17 (-0.54, 0.73) | -0.28 (-0.66, 0.90) |
| PM ₁₀ particulate | 0.49 (0.27, 0.73) | 0.05 (-0.08, 0.27) | -0.30 (-0.49, 0.07) |
| PM _{2.5} particulate | 0.45 (-0.11, 0.71) | 0.12 (-0.03, 0.30) | -0.17 (-0.38, 0.22) |
| Sulphur dioxide, SO ₂ | 0.32 (0.09, 0.59) | 0.29 (0.13, 0.39) | 0.30 (0.17, 0.51) |

654 In bold, the significant cases according to the deterministic terms. In parenthesis, the 95% confidence
 655 intervals of the values of d.

656

657

658 **Table 5: Estimates of d under the assumption of seasonal autocorrelation**

| London mean roadside | | | |
|-------------------------------------|-------------------|--------------------------|---------------------------|
| Series | No terms | With intercept | With a time trend |
| Nitric oxide, NO | 0.72 (0.54, 0.95) | 0.60 (0.41, 0.91) | 0.60 (0.39, 0.91) |
| Nitrogen dioxide, NO ₂ | 0.79 (0.66, 0.96) | 0.36 (0.23, 0.56) | 0.32 (0.16, 0.54) |
| Oxides of nitrogen, NO _x | 0.74 (0.57, 0.96) | 0.54 (0.33, 0.86) | 0.53 (0.32, 0.86) |
| Ozone, O ₃ | 0.55 (0.40, 0.75) | 0.24 (0.09, 0.50) | 0.25 (0.10, 0.50) |
| PM ₁₀ particulate | 0.52 (0.39, 0.68) | 0.14 (0.03, 0.29) | 0.08 (-0.06, 0.27) |
| PM _{2.5} particulate | 0.42 (0.28, 0.58) | 0.16 (0.05, 0.32) | 0.06 (-0.10, 0.27) |
| Sulphur dioxide, SO ₂ | 0.44 (0.30, 0.60) | 0.30 (0.17, 0.46) | 0.28 (0.14, 0.46) |
| London mean background | | | |
| Series | No terms | With intercept | With a time trend |
| Nitric oxide, NO | 0.59 (0.36, 0.88) | 0.47 (0.25, 0.85) | 0.46 (0.19, 0.85) |
| Nitrogen dioxide, NO ₂ | 0.77 (0.62, 0.96) | 0.34 (0.22, 0.53) | 0.20 (0.00, 0.50) |
| Oxides of nitrogen, NO _x | 0.68 (0.48, 0.94) | 0.47 (0.25, 0.85) | 0.46 (0.19, 0.85) |
| Ozone, O ₃ | 0.52 (0.34, 0.74) | 0.27 (0.12, 0.52) | 0.26 (0.09, 0.53) |
| PM ₁₀ particulate | 0.45 (0.31, 0.61) | 0.12 (-0.03, 0.28) | 0.04 (-0.11, 0.25) |
| PM _{2.5} particulate | 0.44 (0.31, 0.60) | 0.26 (0.13, 0.44) | 0.21 (0.05, 0.42) |
| Sulphur dioxide, SO ₂ | 0.45 (0.31, 0.60) | 0.28 (0.18, 0.42) | 0.28 (0.18, 0.42) |

659 In bold, the significant cases according to the deterministic terms. In parenthesis, the 95% confidence
660 intervals of the values of d.

661

662

663 **Table 6: Estimates of d under the assumption of seasonal autocorrelation**

| London mean roadside | | | | |
|-------------------------------------|--------------------|----------------|----------------|-------|
| Series | d (95% interval) | Intercept | Time trend | AR |
| Nitric oxide, NO | 0.60 (0.41, 0.91) | 84.921 (5.54) | --- | 0.354 |
| Nitrogen dioxide, NO ₂ | 0.32 (0.16, 0.54) | 60.442 (19.15) | -0.080 (-1.99) | 0.428 |
| Oxides of nitrogen, NO _x | 0.54 (0.33, 0.86) | 143.642 (8.51) | --- | 0.420 |
| Ozone, O ₃ | 0.24 (0.09, 0.50) | 27.478 (14.20) | --- | 0.669 |
| PM ₁₀ particulate | 0.08 (-0.06, 0.27) | 28.009 (25.18) | -0.044 (-3.10) | 0.382 |
| PM _{2.5} particulate | 0.06 (-0.10, 0.27) | 18.819 (19.38) | -0.047 (-3.76) | 0.286 |
| Sulphur dioxide, SO ₂ | 0.30 (0.17, 0.46) | 3.410 (8.52) | --- | 0.203 |
| London mean background | | | | |
| Series | d (95% interval) | Intercept | Time trend | AR |
| Nitric oxide, NO | 0.47 (0.25, 0.85) | 26.871 (4.02) | --- | 0.359 |
| Nitrogen dioxide, NO ₂ | 0.20 (0.00, 0.50) | 41.813 (17.55) | -0.101 (-3.40) | 0.646 |
| Oxides of nitrogen, NO _x | 0.47 (0.25, 0.85) | 66.240 (6.46) | --- | 0.429 |
| Ozone, O ₃ | 0.27 (0.12, 0.52) | 37.105 (13.76) | --- | 0.692 |
| PM ₁₀ particulate | 0.04 (-0.11, 0.25) | 21.795 (24.58) | -0.038 (-3.32) | 0.646 |
| PM _{2.5} particulate | 0.21 (0.05, 0.42) | 15.642 (10.77) | -0.038 (-2.04) | 0.646 |
| Sulphur dioxide, SO ₂ | 0.28 (0.18, 0.42) | 3.332 (13.20) | --- | 0.230 |

664 In parenthesis in the second column, the 95% confidence intervals of the estimated values of d. in the third
 665 and fourth column, t statistics values are in parenthesis. The “AR” is the estimated seasonal AR(1) values.
 666

667
 668
 669
 670
 671
 672
 673
 674
 675

Table 7: Results of the HEGY Quarterly Seasonal unit root

| i) London mean roadside | | | | |
|-------------------------------------|-------------------------------------|---------------|----------------|----------------|
| Series | Regression | t_1 | t_2 | F_{2-12} |
| Nitric oxide, NO | Intercept only | 0.2429 | -0.8343 | 7.9221 |
| | Intercept and trend | -0.7950 | -0.8413 | 7.7816 |
| | Intercept, trend and seasonal dummy | 0.8748 | 0.5871 | 13.8999 |
| Nitrogen dioxide, NO ₂ | Intercept only | -0.7176 | -0.8088 | 6.1134 |
| | Intercept and trend | -2.3521 | -0.8124 | 6.1146 |
| | Intercept, trend and seasonal dummy | 2.8932 | 2.9362 | 9.9875 |
| Oxides of nitrogen, NO _x | Intercept only | -0.8530 | -0.6957 | 7.5510 |
| | Intercept and trend | -1.8307 | -0.6930 | 7.4601 |
| | Intercept, trend and seasonal dummy | 2.6703 | 2.6227 | 14.6369 |
| Ozone, O ₃ | Intercept only | -1.2149 | -1.8058 | 4.5338 |
| | Intercept and trend | -1.6516 | -1.8080 | 4.4319 |
| | Intercept, trend and seasonal dummy | 3.6920 | 3.5954 | 10.5347 |
| PM ₁₀ particulate | Intercept only | -0.2150 | -0.8383 | 5.0926 |
| | Intercept and trend | -2.8297 | -0.6235 | 5.0243 |
| | Intercept, trend and seasonal dummy | 3.2142 | 3.2061 | 6.9362 |
| PM _{2.5} particulate | Intercept only | -0.0164 | -0.7408 | 4.9104 |
| | Intercept and trend | -1.9584 | -0.6437 | 4.8029 |
| | Intercept, trend and seasonal dummy | 2.4029 | 2.4659 | 7.7611 |
| Sulphur dioxide, SO ₂ | Intercept only | 1.3854 | -0.8968 | 5.3395 |
| | Intercept and trend | 0.3269 | -0.8863 | 4.9650 |
| | Intercept, trend and seasonal dummy | 1.3805 | 1.6499 | 5.8573 |
| ii) London mean background | | | | |
| Series | Regression | t_1 | t_2 | F_{2-12} |
| Nitric oxide, NO | Intercept only | 1.4599 | -0.7625 | 6.8367 |
| | Intercept and trend | 0.5360 | -0.7741 | 6.8876 |
| | Intercept, trend and seasonal dummy | -0.1487 | -0.2389 | 12.0501 |
| Nitrogen dioxide, NO ₂ | Intercept only | 0.9932 | -0.5471 | 5.5080 |
| | Intercept and trend | -0.8502 | -0.5334 | 5.4032 |
| | Intercept, trend and seasonal dummy | 1.5246 | 1.6500 | 8.1662 |
| Oxides of nitrogen, NO _x | Intercept only | 0.4292 | -0.5903 | 6.6705 |
| | Intercept and trend | -0.1071 | -0.6044 | 6.6629 |
| | Intercept, trend and seasonal dummy | 0.9679 | 0.8257 | 12.3667 |
| Ozone, O ₃ | Intercept only | -1.9739 | -1.3880 | 3.6973 |
| | Intercept and trend | -1.9417 | -1.3786 | 3.6504 |
| | Intercept, trend and seasonal dummy | 3.9302 | 3.7862 | 10.5785 |
| PM ₁₀ particulate | Intercept only | 0.3369 | -0.8042 | 4.7729 |
| | Intercept and trend | -3.0612 | -0.6396 | 4.6386 |
| | Intercept, trend and seasonal dummy | 3.4327 | 3.4149 | 6.6551 |
| PM _{2.5} particulate | Intercept only | 0.1899 | -0.6368 | 5.5896 |
| | Intercept and trend | -2.4430 | -0.4708 | 5.4172 |
| | Intercept, trend and seasonal dummy | 3.1601 | 3.2390 | 8.3624 |
| Sulphur dioxide, SO ₂ | Intercept only | -0.9885 | -2.3177 | 5.6763 |
| | Intercept and trend | -0.9644 | -2.2991 | 5.5756 |
| | Intercept, trend and seasonal dummy | 2.4293 | 2.0294 | 7.4713 |

677
678
679
680
681

In bold in the column for t statistic t_1 indicates evidence of no regular unit root at 5% level, while in bold for a column for t statistic t_2 indicates evidence of no seasonal unit roots at annual frequency, vice-versa. In the last column, the joint F tests F_{2-12} are reported with Estimates in bold implying no evidence of seasonal unit roots at all other frequencies other than annual frequency. Critical values of the test are given in Franses and Hobijn (1997).

682
683

Table 8: Estimates based on a non-linear I(d) model with white noise errors

| i) London Mean Roadside | | | | | |
|-------------------------------------|-----------------------|---------------------------------|-------------------------------|---------------------------------|-------------------------------|
| Series | d | θ_0 | θ_1 | θ_2 | θ_3 |
| Nitric oxide, NO | 0.73 (0.47, 1.01) | 86.585 (2.31) | 9.415 (0.44) | -11.400 (-0.80) | 5.712 (0.53) |
| Nitrogen dioxide, NO ₂ | 0.46 (0.25, 0.68) | 55.833 (13.20) | 2.918 (1.12) | -1.845 (-0.87) | 1.015 (0.56) |
| Oxides of nitrogen, NO _x | 0.72 (0.47, 0.99) | 150.178 (3.30) | 6.606 (0.25) | -7.393 (-0.42) | 3.911 (0.29) |
| Ozone, O ₃ | 0.74 (0.51, 0.98) | 27.362 (1.91) | 0.668 (0.08) | 0.045 (0.01) | 0.828 (0.20) |
| PM ₁₀ particulate | 0.11 (-0.09, 0.37) | 25.152 37.06 | 1.692 (2.85) | -0.968 (-1.71) | -1.816 (-0.03) |
| PM _{2.5} particulate | 0.11 (-0.08, 0.35) | 15.717 (24.53) | 1.797 (3.21) | -0.294 (-0.55) | -0.004 (-0.09) |
| Sulphur dioxide, SO ₂ | 0.28 (0.12, 0.48) | 86.585 (2.31) | 9.415 (0.44) | -11.400 (-0.80) | 5.712 (0.53) |
| ii) London Mean Background | | | | | |
| Series | d | θ_0 | θ_1 | θ_2 | θ_3 |
| Nitric oxide, NO | 0.67 (0.40, 0.97) | 27.937 (1.78) | 4.822 (0.48) | -0.990 (-0.13) | 2.534 (0.46) |
| Nitrogen dioxide, NO ₂ | 0.68 (0.45, 0.93) | 36.407 (3.45) | 3.852 (0.64) | 0.564 (0.13) | 0.784 (0.24) |
| Oxides of nitrogen, NO _x | 0.74 (0.47, 1.02) | 71.022 (2.00) | 7.532 (0.37) | 1.332 (0.10) | 2.748 (0.27) |
| Ozone, O ₃ | 0.83 (0.60, 1.07) | 36.431 (1.85) | -0.300 (-0.02) | 0.219 (0.02) | 0.527 (0.07) |
| PM ₁₀ particulate | 0.09 (-0.11, 0.34) | 19.281 33.77 | 1.486 (2.91) | -0.324 (-0.66) | -0.203 (-0.42) |
| PM _{2.5} particulate | 0.24 (0.04, 0.49) | 13.277 (12.71) | 1.557 (1.98) | -0.418 (-0.59) | -0.309 (-0.47) |
| Sulphur dioxide, SO ₂ | 0.15 (0.00, 0.35) | 3.373 (23.85) | 0.146 (1.24) | -0.438 (-3.96) | 0.224 (2.12) |

684 In parenthesis in the second column, the 95% confidence interval for d. In the third to the sixth column are
685 t-values for parameters θ_0 , θ_1 , θ_2 and θ_3 , respectively. Figures in bold indicate the significance of estimates
686 at 5% level.
687

688
689
690